CZECHOSLOVAK ACADEMY OF SCIENCES

CZECHOSLOVAK JOURNAL OF PHYSICS

REPRINT

VOLUME B 38

1988

MAGNETIC DIAGNOSTICS ON THE CASTOR TOKAMAK

M. Valovič

Institute of Plasma Physics, Czech. Acad. Sci., Pod vodárenskou věží 4, 182 11 Praha 8, Czechoslovakia

Plasma position and Shafranov eccentricity factor is measured on the CASTOR tokamak using magnetic probes. Evolution of eccentricity factor is illustrated on discharge with auxiliary non-inductive current-drive by lower hybrid waves.

1. INTRODUCTION

Magnetic measurement of the plasma position in tokamaks with a circular cross-section is based on the Shafranov analytical expression for poloidal magnetic field around the plasma in the MHD equilibrium [1]. Measuring this field the eccentricity factor $\Lambda = \beta_p + \frac{1}{2}l_i$ can also be determined. Here β_p denotes poloidal beta and l_i coefficient of internal inductance. The plasma position refers to the centre of the cross-section of plasma boundary. The boundary is defined as the magnetic surface on which plasma pressure is zero. In a real experiment it is represented by the outermost surface which does not yet intersect the limiters. Moreover, it is assumed that during the displacement its circular shape is not deformed.

One of the possible techniques how to determine the above parameters is to measure the local values of poloidal magnetic field at four points around the plasma and an average vertical magnetic field in the vacuum chamber [2]. This method is used in the present paper.

2. DIAGNOSTICS

CASTOR tokamak has radius $R_0 = 0{\cdot}4$ m and radius of circular limiter aperture $a_L = 85$ mm. In this experiment, toroidal magnetic field was $B_T = 1{\cdot}3$ T. Basic elements of the poloidal magnetic field system are shown in fig. 1. The iron-core transformer has two limbs. The vacuum vessel is surrounded by 10 mm thick copper shell with inner radius of 117 mm. There are six diagnostic ports so that 14% of the plasma length is not shielded. Outside of the shell are placed two external quadruple coil systems which generate static vertical B_V and horizontal B_H magnetic fields, One internal system inside a shell generates vertical field proportional to the primary current.

The scheme of the measurement is shown in fig. 1. The signals are taken from seven diagnostic coils (tab. 1). Plasma current I_p is measured by a Rogowski coil wound outside the shell. Poloidal magnetic fields $B_\omega(\varphi)$ are determined by Mirnov coils placed at minor radius $b = 110$ mm ($\varphi = 0, \frac{1}{2}\pi, \pi$ and $-\frac{1}{2}\pi$ for outer, upper, inner and lower coils resp.). An average vertical magnetic field along the torus

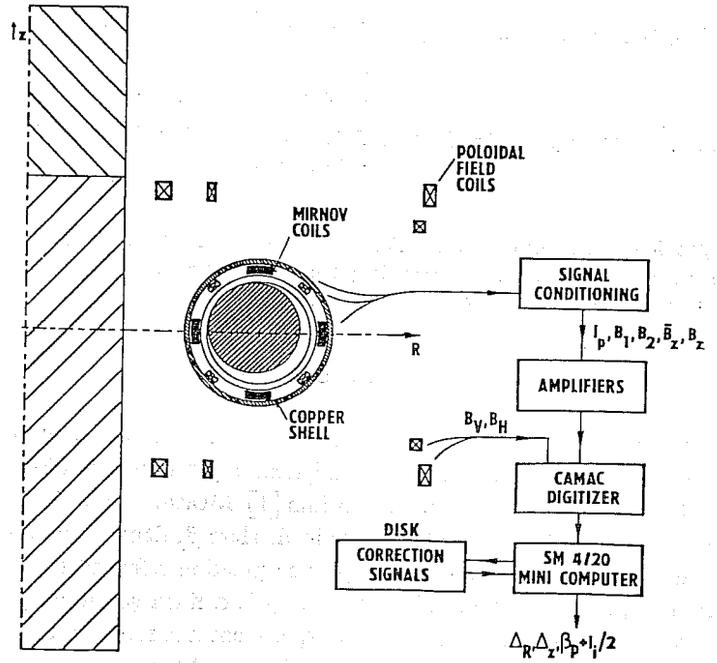

Fig. 1. CASTOR tokamak poloidal field system and block diagram of the magnetic measurement.

$\bar{B}_z$ is measured by two loops at $R = R_0 \pm b$, $z = 0$. One of these loops also determines the loop voltage U_L. One saddle coil measures the local vertical magnetic field B_z in the cross-section of the Mirnov coils.

Table 1.

Diagnostic summary.

Coil		Sensitivity
Rogowski		$3{\cdot}5 \times 10^6$ A/Vs
Mirnov	$\varphi = 0$	4·0 T/Vs
	π	7·9 T/Vs
	$\frac{1}{2}\pi$	7·2 T/Vs
	$-\frac{1}{2}\pi$	6·5 T/Vs
$\bar{B}_z$ loops		1·7 T/Vs
saddle		6·5 T/Vs

The signals from coils are weighted, summed and passively integrated. This conditioning also includes rough compensation of errors from toroidal magnetic field. The signals together with values of static fields are then digitized in the CAMAC and processed in minicomputer. In the first step, toroidal field is eliminated using correction data stored on a disk memory. In a second step, eccentricity, horizontal Δ_R and vertical Δ_z displacements are determined from Shafranov equations:

$$(1)\qquad \begin{aligned} \Lambda &= \left(\frac{B_1}{2} - \bar{B}_z\right)\frac{R_0}{B_0 b} - \ln\frac{b}{a} + 1 \\ \Delta_R &= \frac{B_1}{2B_0}\,.\,b - \tfrac{1}{2}\left[\ln\frac{b}{a} - 1 + (\Lambda - \tfrac{1}{2})\left(1 + \frac{a^2}{b^2}\right)\right]\frac{b^2}{R_0} \\ \Delta_z &= \frac{B_2}{2B_0}\,.\,b \\ a &= a_L - (\Delta_R^2 + \Delta_z^2)^{1/2}\,. \end{aligned}$$

Here $B_1 = B_\omega(\pi) - B_\omega(0)$, $B_2 = B_\omega(-\frac{1}{2}\pi) - B_\omega(\frac{1}{2}\pi)$, $B_0 = \mu_0 I_p/2\pi b$, $\mu_0 = 4\pi \times 10^{-7}$ H/m. It is assumed that $|\Lambda - 1|.\, a/R_0 \ll 1$, $\Delta_R \ll b$ and $\Delta_z \ll b$. The system (1) is solved iteratively with the first guess $a = a_L$ until the relative change of a is less than 1%. Thus an absolute numerical error of $\pm 0{\cdot}01$ in Λ and $\pm 0{\cdot}1$ mm in Δ_R is ensured.

In formulas (1) the modulation of the poloidal magnetic field along the torus is not considered. In CASTOR tokamak, however, it is substantial. The modulation is produced by the limbs of the transformer and by the diagnostic windows in the copper shell. In this case the local value B_1 in equations (1) must be replaced by its averaged $\bar{B}_1$ along the torus. If the modulation is small it can be simply determined as [3]:

$$\bar{B}_1 = B_1 + 2(B_z - \bar{B}_z)\,.$$

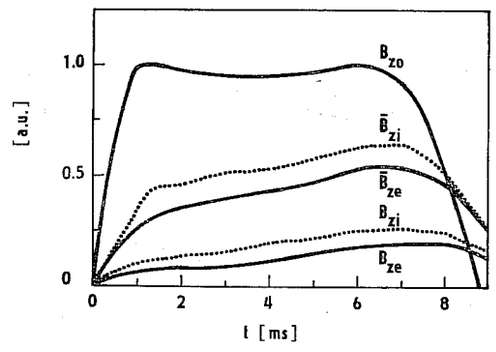

Fig. 2. Diffusion of the vertical magnetic field through the copper shell: B_{z0} — current in the quadruple coil systems normalized to the magnetic field in the vacuum chamber, $\bar{B}_{zi}$, $\bar{B}_{ze}$, B_{zi}, B_{ze} — fields measured by loops and saddle coil, respectively (indices i, e refer to the fields generated by internal and external coils, respectively).

We made some attempt to find the modulation caused by the copper shell. The results are summarized in fig. 2. Both external and internal vertical field coils were charged by a pulse from the primary current power supply. It is seen from waveforms of $\bar{B}_z$ and B_z that during the plateau $B_z/\bar{B}_z \approx 0{\cdot}3-0{\cdot}4$. Note that even at the beginning $\bar{B}_z$ is about $(30-40)\%$ of its full value. Therefore physically much more of the plasma length remains unshielded than it is determined from the geometry of the windows.

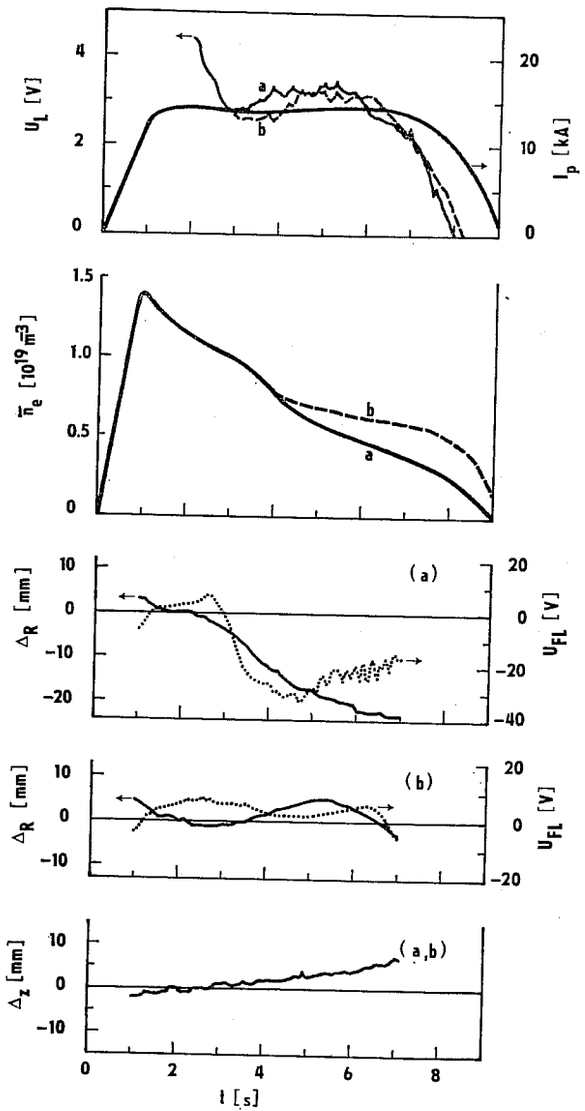

Fig. 3. Magnetic data from ohmic discharges without (a) and with (b) improved vertical equilibrium field.

3. PERFORMANCE

An example of the magnetic measurements on ohmic discharge without gas puffing is shown in fig. 3a. The most remarkable observation is the inward movement of the plasma column. This magnetically determined plasma position was cross-checked by a simple method using the floating potentials of the limiters. CASTOR tokamak has two C-shaped limiter segments divided by a vertical gap. If $\Delta_R = 0$, inner and outer limiters have the same floating potentials. For $\Delta_R > 0$, outer limiter is immersed in the plasma with higher electron temperature than inner one and thus the potential difference between inner and outer limiters, ΔU_{FL}, is positive and vice versa. By this method the position $\Delta_R = 0$ is justified with an accuracy of 5 mm and also an inward movement of the plasma is confirmed.

A better plasma position is obtained when time-dependent vertical magnetic field is applied instead of B_v. Such shot is presented in fig. 3b. Slower fall of the line averaged electron density $\bar{n}_e$ shows improved particle confinement.

Upward plasma movement is the feature of all discharges. Applying various B_H alters only the bias but not this tendency. It is caused by a horizontal component

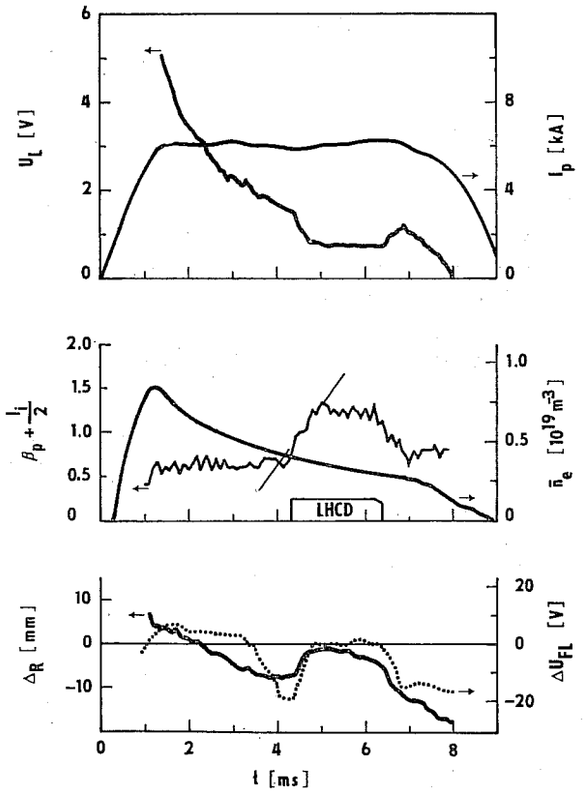

Fig. 4. Magnetic data from ohmic discharge with auxiliary lower-hybrid-current-drive (LHCD).

of the stray magnetic field which is produced by an asymmetrically placed air gap in the iron core.

Further magnetic data were taken from ohmic discharge with auxiliary non-inductive current-drive. In these experiments electromagnetic power from magnetron (40 kW, 1·25 GHz) is launched into the plasma via a phased waveguide array to excite lower hybrid waves with a mean phase velocity directed along the torus. The momentum of the waves is transferred to the electrons by Landau damping and thus non-inductive current is driven. For details of lower-hybrid-current-drive (LHCD) on CASTOR tokamak see [4].

Evolution of eccentricity factor during LHCD is shown in fig. 4. Its large increase $\Delta\Lambda \approx 0{\cdot}6$ with initial rate of rise $\dot{\Lambda} \approx 1{\cdot}6 \times 10^3\ \mathrm{s}^{-1}$ is caused only by the change of β_p because of logarithmic dependence of l_i on the plasma current profile. From $\Delta\beta_p$ a mean longitudinal velocity of electrons accelerated by the wave can be estimated by:

$$v_{\parallel} \equiv \frac{\mu_0 e}{4\pi m} \Delta\beta_p \frac{I_p^2}{I} \approx 7 \times 10^7\ \mathrm{m/s}\ .$$

Here I is noninductive current determined from the voltage drop ΔU_L: $I = I_p\, \Delta U_L : U_L \approx 3\ \mathrm{kA}$, e and m are electron charge and mass. This value is approximately equal to the phase velocity of the wave. Absorbed power corresponding to $\dot{\beta}_p$ is $P \approx 7\ \mathrm{kW}$. Since the current-drive efficiency is

$$\gamma = \frac{IR_0\langle n_e\rangle}{P} \approx 0{\cdot}05 \times 10^{19}\ \mathrm{A\,m^{-2}\,W^{-1}}\ ,$$

where $\langle n_e\rangle = 0{\cdot}75\bar{n}_e \approx 0{\cdot}24 \times 10^{19}\ \mathrm{m^{-3}}$ is volume averaged electron density. This value is in good agreement with observed efficiencies [5] (central electron temperature estimated from Spitzer conductivity is 200 eV in our experiment). It must be noted, however, that such good consistency between $\Delta\Lambda$ and ΔU_L is not obtained for another Δ_R. It can be explained by the well known sensitivity of the antenna space spectrum on the density profile at the plasma edge.

4. CONCLUSION

Magnetic measurements on the CASTOR tokamak showed that a careful control of the plasma position, especially during the current-drive experiments, is necessary. From evolution of $\beta_p + \frac{1}{2}l_i$ during the non-inductive current-drive useful information can be drawn.

Author thanks to Dr. Kopecký for his support. The members of the CASTOR group are gratefully acknowledged, especially Dr. Kryška for his introduction into the CAMAC operation.

Received 10. 12. 1986.

References

[1] Mukhovatov V. S., Shafranov V. D.: Nuclear Fusion *11* (1971) 605.
[2] Shafranov V. D.: *in* Voprosy teorii plazmy, Vol. 11. Energoizdat, Moscow, 1982.
[3] Zacharov L. E., Shafranov V. D.: Zh. Tekh. Fiz. *48* (1978) 1156.
[4] Nanobashvili S., Badalec J., Ďatlov J., Jakubka K., Kopecký V., Körbel Š., Kryška L., Magula P., Stöckel J., Valovič M., Žáček F.: Fiz. Plazmy — to be published.
[5] Ehst D. *in* Proc. IAEA INTOR-related Specialists' Meeting on Noninductive Current Drive, Garching (BRD) 1986, p. 15.